International Conference on Renewable Energies and Power Quality (ICREPQ'13)
Bilbao (Spain), 20th to 22th March, 2013
Renewable Energy and Power Quality Journal (RE&PQJ)
ISSN 2172-038 X, No.11, March 2013

Modeling and Control of Micro Grid Powered by Maximum Power PV Array and Fixed Speed Wind Energy Conversion System

M.M.A.Mahfouz[1] and Mohamed A. H. El-Sayed[2]

[1] Department of Electrical Power and Machines
Faculty of Engineering, Helwan University, Cairo, Egypt
Phone: +2 0100 9708055, E-mail: mohamed.mahfouz@yahoo.co.uk

[2] Colleges of Engineering and Petroleum, Kuwait University, Kuwait
Phone: +965 24983347, E-mail: elsmah@hotmail.com

Abstract. In this paper, the dynamic modeling of the studied micro grid (MG) is presented for steady state and transient operation conditions. Moreover, control strategies to obtain the maximum converted power and stabilize the voltage under different operating conditions are derived. The integrated system under study has four key subsystems to supply the required electric loads. The first and second subsystems include the layout of the studied MG and the renewable generation sources from Wind turbine and PV array. The third represents the boost converter between the PV and the DC collection bus as well as the interfaced inverter to the point of common coupling (PCC) with the MG. The fourth subsystem comprises mainly the required PI controllers to regulate the modulation index of the inverter and the duty cycle of the boost converter for PV maximum in addition of regulating the boost inverter DC link voltage. The proportional and integral parameters of these controllers are tuned off-line to enhance the grid performance. The integrated system and the associated subsystems are fully validated for efficient operation under normal or fault conditions using the Matlab/Simulink/Sim-Power software.

Key words
Micro Grid, Photovoltaic (PV) array, Wind energy conversion, DC/DC boost converter, Inverter (VSI)

1. Introduction

Distributed generation (DG) is becoming an important research area to facilitate the utilization of green energy resources. Compared with conventional power plants, distributed generation has less pollution and high reliability. Moreover, installation of DG energy resources can potentially postpone the demand for distribution and transmission expansion planning to cover the increasing electric demand of the consumers [1]. Interconnection of different DG units to distribution network forms a new system called MG. MGs with DG close to load centers will reduce the required power flows from transmission and distribution networks resulting in loss reduction and reliability increase. Micro grids will reduce also the harmful gas emission and mitigate climate changes. This is attributed to the fact that the installed DG units are based on renewable sources that are free emissions [2].

Distributed generations used in micro grids are technically not suitable for direct energy supply to the grid. They have to be interfaced with Micro Grid through power conditioning devices and appropriate control strategies in order to provide the required voltage and frequency at PCC [3]. Wind turbine will generally operate in normal conditions with voltage level between 90 and 105% and frequency between 49-51 Hz. The penetration of distributed generation may violate these operation constraints. Therefore, the active and reactive power supplied to the distribution network should be continuously controlled to regulate the voltage and frequency of the system. Under fault conditions, the wind turbine would experience large voltage variations. The amplitude and duration of these variations will determine whether the wind turbine should be disconnected or kept in operation during fault conditions. MG can provide the required reactive power for voltage regulation and assist wind farms to continue in supplying active power for certain time during fault conditions [4].The main objective of this paper is to study the steady state and transient behavior of MG under varying loads and climate conditions. In order to assess system behavior a complete model will be developed to simulate the MG's components including power conditioning system. Maximum power is tracked under time varying wind speed and solar radiation. The developed model was built in Matlab/Simulink environment. The layout of the studied MG is presented in Section 2 together with a brief description of wind and solar energy driven DG units.

Section 3 and 4 present the description of the boost converter and the interfaced inverter with their proposed control strategies. The studied cases with results and discussions are explained in Section 5. Conclusions are summarized in Section 7.

2. Micro grid System Components and Modeling

A single line diagram of the micro grid system studied in this paper is illustrated in Fig. 1. It consists of 22 kV network, 600 kW wind turbine and 200 kW PV panel. The average wind speed is 10 m/s at 40 m above ground level. The wind turbines are connected to the network through 800kVA, 690V/22kV transformers. The turbines are coupled to induction generators and have fixed capacitors, rated speed of 12 m/s. Local loads are included in the system with total active and reactive power of 400 kW and 100kVAR, respectively. The PV arrays are connected to the grid through DC/DC boost converter and DC/AC 3-phase two-level inverter. After inversion the arrays are interfaced to the distribution network through 6 kV/22 kV transformer. In the case of installing fixed capacitor for induction generator excitation, the system may need additional source of reactive power from the grid to enhance system performance.

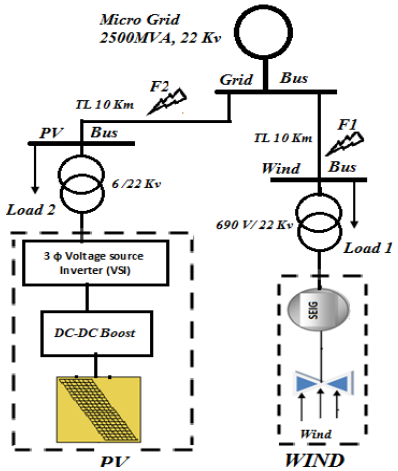

Fig.:1 Layout of the studied micro grid

A. Fixed Speed Wind Turbine with Induction Generator

The extracted power of wind turbine depends on three main factors: available wind power, the power curve of the machine and the ability of the machine's response to wind fluctuation. The expression for power produced by the wind is given by [5]:

$$p_a = \varpi_r T_w = \frac{1}{2}\rho . A . C_p(\lambda, \beta) . V_w{}^3 \quad (1)$$

Where;

Pa is the aerodynamic power, *Cp(λ, β)* is the dimensionless aerodynamic power performance coefficient, ρ*=1.25 kg/m3* is the air density, $A=\pi R^2$is the rotor swept area, V_w is the wind speed, ω is the blade rotating speed, λ is the tip-speed ratio and β represents pitch angle. The tip speed ratio is defined as:

$$\lambda = \varpi \frac{R}{V_w} \quad (2)$$

Where; ω is the rotor speed and R is the rotor radius. The wind turbine can be characterized by its (C_P– λ).It is seen that if the rotor speed is kept constant, then any change in the wind speed will change the tip-speed ratio, leading to the change of power coefficient C_p as well as the generated power. If, however, the rotor speed is adjusted according to the wind speed variation, then the tip-speed ratio can be maintained at an optimal point, which could yield maximum power output from the system.

For the modeling of the wind turbine the power coefficient Cp(λ, β) of eq. (3) is used, which represents the fraction of the power in the wind captured by the turbine and has a theoretical maximum of 0.55 [6].

$$C_p = \frac{1}{2}(\gamma - 0.022\,\beta^2 - 5.6)e^{-0.17\gamma} \quad (3)$$

The pitch control system is one of the most widely used control techniques to regulate the output power of a wind turbine generator. The method relies on the variation in the power captured by the turbine as the pitch angle of the blades is changed.

B. Photovoltaic Array

Using the physics of p-n junctions, a PV cell can be modeled as a DC current source in parallel with a diode that represents the most effective current escaping due to diffusion mechanisms. Two resistances, R_s and R_p, are included to model the contact resistances and internal PV cell resistance respectively. A solar cell equivalent circuit is usually represented [7], as shown in Fig. 2.

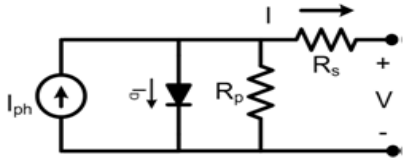

Fig. 2: Solar cell equivalent circuit

The current source I_{ph} represents the photocurrent of the cell. The relationships between the PV cell output current and terminal voltage is given by:

$$I = I_{ph} - I_{rs}\left[\exp\left(\frac{q(V+IR_s)}{AKT}\right) - 1\right] - \frac{V+IR_s}{R_p} \quad (4)$$

Where; *A* is the diode ideality factor, *k* is the Boltzmann constant ($1.3806503 \times 10^{-23}$ J/K), *T* is the cell temperature in Kelvin, *q* is the electron charge ($1.60217646 \times 10^{-19}$ C), I_{rs} is the reverse saturation currents of the diode, respectively. PV cells are grouped in larger units called PV modules, which are further interconnected in a parallel-series configuration to form PV arrays or PV generators. Assuming high value of R_p then for an array with N_s series and N_p parallel-connected cells, the array current may be related to the array voltage as [7, 8]:

$$I = N_p \left[I_{ph} - I_{rs} \left(\exp\left(\frac{q(V+IR_S)}{AKTN_S} \right) - 1 \right) \right] \quad (5)$$

Where:

$$I_{rs} = I_{rr} \left(\frac{T}{T_r} \right)^3 \exp\left[\frac{E_G}{AK} \left(\frac{1}{T_r} - \frac{1}{T} \right) \right] \quad (6)$$

Where; $I_{rs}$is the cell reverse saturation current at temperature T, while T_r is the cell reference temperature, I_{rr} is the reverse saturation current at T_r and E_G is the band gap energy of the semiconductor used in the cell. The photocurrent I_{ph} depends on the cell's temperature and radiation as follows:

$$I_{ph} = [I_{SCR} + k_i(T - T_r)] \frac{S}{100} \quad (7)$$

Where, I_{SCR} is the cell short circuit current at reference temperature and radiation, k_i is the short circuit current temperature coefficient and S is the solar radiation in mW/cm^2. The PV studied system consists of 33 series and 119 parallel modules. Photovoltaic cells vary their voltage output with irradiance, temperature, and current loading [9].

3. Power Conditioning System

The main purpose of a grid-connected PV solar system is to transfer the maximum power obtained from the PV panel into the MG independently of the climatic conditions. Therefore, the use of an appropriate electronic interface with maximum power point tracking (MPPT) capabilities is required.

A. Boost Converter:

A boost converter is a power converter with an output DC voltage greater than its input DC voltage. By implementing the PWM technique on boost converter, a stable output voltage from a non-stable input voltage can be obtained by changing the duty cycle (d) of the switched input pulse. The boost converter is given in Fig. 3 with a switching period T and a duty cycle d. Again, assuming continuous conduction mode of operation, the state space equations when the main switch is ON are shown by, [10].

$$\begin{cases} \frac{di_L}{dt} = \frac{1}{L}(V_{in}) \\ \frac{dv_o}{dt} = \frac{1}{C}(-\frac{v_o}{R}) \end{cases}, \quad 0 < t < dT, \quad Q : ON \quad (8)$$

And when the switch is OFF

$$\begin{cases} \frac{di_L}{dt} = \frac{1}{L}(V_{in} - v_o) \\ \frac{dv_o}{dt} = \frac{1}{C}(i_L - \frac{v_o}{R}) \end{cases}, \quad dT < t < T, \quad Q : OFF \quad (9)$$

The relationship between output V_o and V_{in} voltage is governed by:

$$\frac{V_0}{V_i} = \frac{T_s}{t_{off}} = \frac{1}{1-d} \quad (10)$$

The boost converter operation to achieve MPP of PV array depends mainly on the switching of the electronic devices.

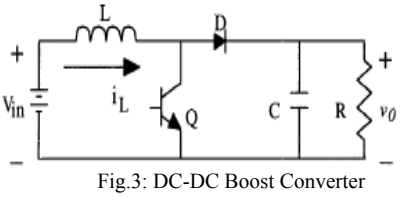

Fig.3: DC-DC Boost Converter

B. PV Array Inverter

The Modular Multilevel inverter (MMI) system has many advantages over conventional voltage source converters [13]. Among various modulation techniques for MMI, PWM is an attractive candidate due to efficient DC link voltage utilization, reducing commutation losses and THD [4,7]. The proposed inverter is a 3-phase, 2-level DC/AC inverter using IGBTs due to their lower switching losses. Depending on the gating signals, the output terminal voltage is either equal to capacitor voltage or zero, and can be expressed by:

$$V_{inv} = N * V_{cap} \quad (11)$$

Where; V_{inv}, N, and $Vcap$ are terminal voltage, gating signal and capacitor voltage, respectively. N takes the value of either one or zero. In the two-level inverter the switching of the upper and lower IGBT generates the output voltages with positive and negative levels (+Vdc and -Vdc). The inverter is generally connected to the network at the PCC through the equivalent inductance and resistance, which represent the impedance of the coupling transformer. The magnetizing inductance of the step-up transformer can also be taken into consideration through a mutual equivalent inductance. The aim of the control strategy is to regulate the current output from the inverter to follow a specified reference value. This can be achieved by transforming the three phase output currents of the inverter to the rotating reference frame (dq0)[11]. The relation between the DC side voltage V_{dc} and the generated AC voltage V_{inv} can be described through the matrix in the *dq*-frame Sav,*dq*, as given by:

$$\begin{bmatrix} V_{inv,d} \\ V_{inv,q} \end{bmatrix} = S_{av,dq} V_{dc} \quad (12)$$

Where; $S_{av,dq} = \frac{\sqrt{3}}{2} m_i$ (13)

And m_i is the inverter modulation index.

4. Proposed Control Scheme

The output power of the PV cell has a nonlinear function with irradiance and temperature. Therefore, the power of the PV array changes continuously and consequently the PV operating point must change to maximize the energy produced. Generally, MPPT techniques can be classified

into direct and indirect groups. Indirect MPPT algorithms are based on calculation of PV cell voltage at maximum power point using sample measurements and there are three operation modes as follows [8, 11];
(i) The operating voltage of PV panel can be adjusted according to the seasonally variable temperature. For example, it is expected that MPP voltage in winter will be higher than summer.
(ii) MPP voltage can be calculated by multiplying the open circuit voltage (V_{oc}) of PV cell with a constant coefficient (0.8for silicon cells).
(iii) In some systems, MPPT algorithms are designed according to the azimuth and altitude of the sun. The advantage of the methods described above is their very simple structures.
On the other side, in the direct algorithms the maximum operating point is determined as follows:
(i) The operating voltage is determined by DC/DC converter to track the maximum module power according to incremental conductance algorithm.
(ii) Second method is the well-known hill-climbing algorithm, where the operating voltage is changed periodically in small steps, and the change in module power is measured. If the power increases depending on the voltage rising of each step, tracking direction is forward, otherwise it is continued backwards [12].

A. MPPT Control Algorithm

The constant voltage (CV) algorithm is the simplest MPPT control method. The operating point of the PV array is kept near the MPP by regulating the array voltage and matching it to a fixed reference voltage $V_{ref.}$ The V_{ref} value is set equal to the V_{MPP} of the PV module. This method assumes that individual insulation and temperature variations on the array are insignificant, and that the constant reference voltage is an adequate approximation of the true MPP. This means that CV algorithm is based on approximately constant ratio between V_{MPP} and V_{oc}as given in eq. (14):

$$V_{MPP} \cong kV_{oc} \quad (14)$$

By the adjusting of array voltage to this calculated value, the operation at MPP is achieved. In literature, K value ranges between 73% and 80% [10]. The measurement of the voltage V_{PV} is necessary in order to set up the duty-cycle of the DC/DC converter. It should be noted that when the PV panel is in low insulation conditions, the CV technique is more effective than either the method of hill-climbing or the incremental conductance. [13].

B. Booster Control

After determining the value for V_{MPP}, the DC/DC boost converter is switched to quickly force the array terminal voltage to itsMPP. The difference between MPP fraction voltage and the array output represents the error of the PI controller, Fig. (4a).This PI controller regulates the PV array voltage by continuously switching on and off of the IGBTs at high frequency according to the varying duty cycle. The fast switching action of the boost converter decouples the dynamics of the PV array due its changes in voltage or current from that of the DC link capacitor, which offers good performance under changing weather conditions. The other advantage of using the boost converter is to increase the array voltage to higher levels suitable for grid interconnection.

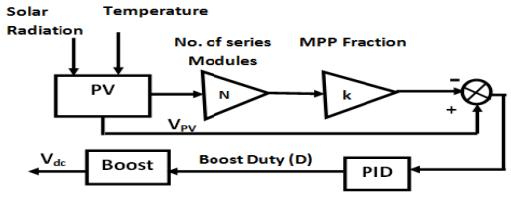

Fig4.a: Boost with MPP block diagrams

C. VSI Inverter Control

A phase locked loop was used to lock on the grid frequency in such a way that V_q was set to zero [8]. If the grid voltage is relatively constant, I_d and I_q can be used to control real and reactive power injections from the PV array. In order to inject real power from the inverter, I_d was controlled using PI controller to follow a specified reference signal I_{d_REF}, reactive power injection was set to zero and thus $I_q = 0$, as displayed in Fig.(4.b). The I_{d_REF} was extracted from the DC link capacitor. A constant DC voltage across the capacitor means that the power that goes into it from the PV array matches the power going out to the inverter [11, 14]. As previously mentioned, the input power $P_{in}$to the capacitor was controlled to be the MPP of the PV array output power by the DC-DC converter. The PI controller was used to extract I_{d_REF} from the error mismatch between Pin and Pout according to the following relation:

$$I_{d\_REF} = \frac{1}{V_d}\left(K_p(P_{in} - P_{out}) + K_I \int (P_{in} - P_{out})dt\right) \quad (15)$$

Where K_P and K_I are the proportional and integral controller constant, respectively and V_d is the direct component of the voltage at PCC. The output of the PI-Controller is Modulation index m, which is fed to PWM switching circuit of Fig. 4.b.

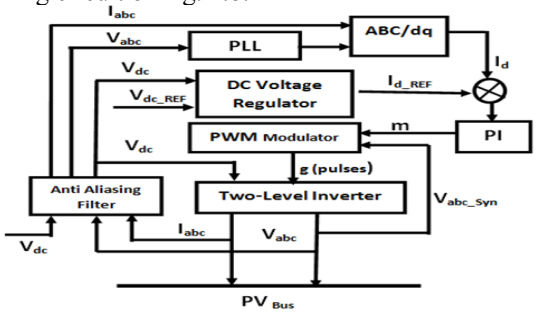

Fig4.b: Block diagram for the Two- level inverter VSI

5. SIMULATION RESULTS

The samples of input wind speed and solar radiation are displayed in Fig. (5). 3-phase fault is applied on the feeders connecting the grid with the two PCC of the wind turbine

and PV array. This fault is initiated at 1.5 s and cleared after 100ms.Due to lack of space selected simulation results are displayed to summarize the system response under normal operation and for a 3-phase fault conditions.

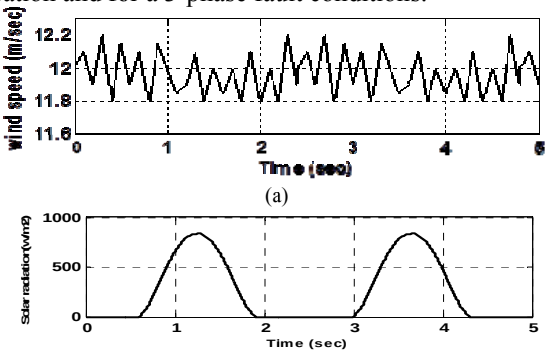

Fig. 5: Time series of the input data (a) wind speed (b) solar radiation

Figure (6) shows the dynamic response of the grid voltage, current, active and reactive power. During the fault condition the current and power supplied by the grid are rapidly increased and return back to its normal value after fault clearing. Similarly, Fig. (7) Shows voltage, current, active and reactive power injected at wind-PCC. During the fault the voltage magnitude at wind-PCC is dropped to 0.75 pu and the injected wind power is consequently decreased.

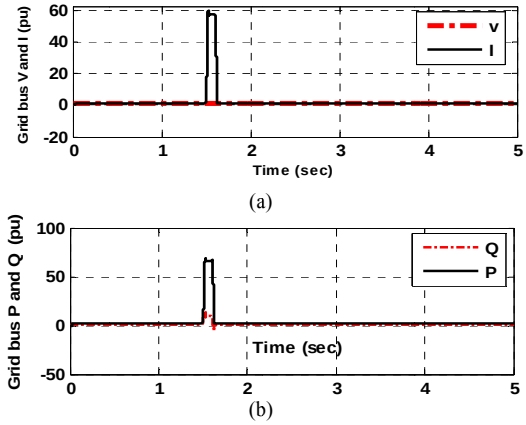

Fig. 6: Dynamic response of the grid variables (a) Voltage and current (b) active and reactive power

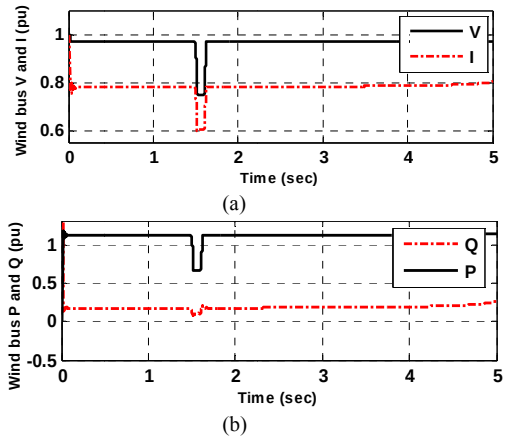

Fig.7: Dynamic response of wind energy conversion system variables at wind-PCC (a) Voltage and current (b) active and reactive power

The PV array generated power is shown in Fig. (8a) corresponding to the input radiation. Comparing the PV array power with the available solar radiation indicated that the PV generated power matches the solar radiation. The MPP for each solar radiation condition is rapidly tracked by the proposed simple CV algorithm. Similarly, Fig. (8b) shows the variations of the voltage and current at PV-PCC. The voltage at the PV-PCC is maintained almost invariant except during the fault it is reduced to zero value. The current response is the same as at the wind-PCC. It is also verified that a very low transient is recording in the exchanged power of the grid-connected PV system due to the proposed full decoupled current control strategy in *d-q* coordinates.

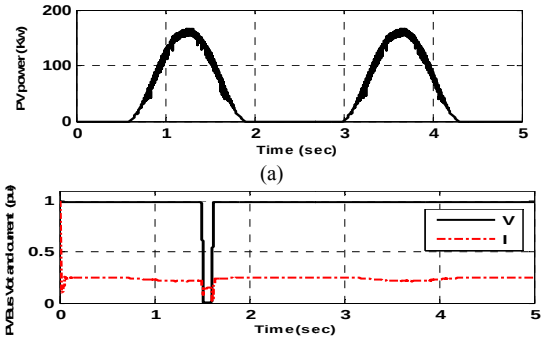

Fig. 8: Dynamic response of the PV array, (a) generated maximum power and (b) voltage and current

The instantaneous value of inverter phase voltage, inverter modulation index m, the DC-link capacitor voltage and the boost converter duty cycle are displayed in Fig. (9) for 3-phase fault at 5 km from PV-PCC. Similar system behavior is obtained for another case with the fault at 5 km from wind-PCC. This can be attributed to the short feeder lengths in micro-grids. As shown in Fig. (7,8), the generating units reached their stable state after tripping the fault. The simulation results validate the robustness of the control scheme for constant speed wind turbine and PV-MPP tracking. The DC link controller regulated the capacitor voltage at approximately 7000 V. The dc link voltage is varied around its set value due to the capacitive charging according to the available daily solar radiation and discharge during night. The modulation index of the VSI is controlled to adjust the magnitude of the instantaneous voltage at the PCC. The duty cycle is adjusted for MPP tracking of the available solar radiation.

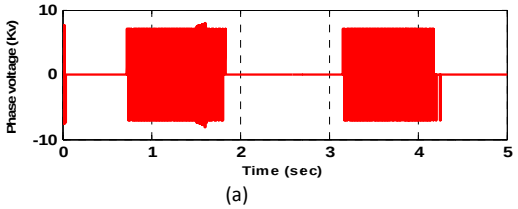

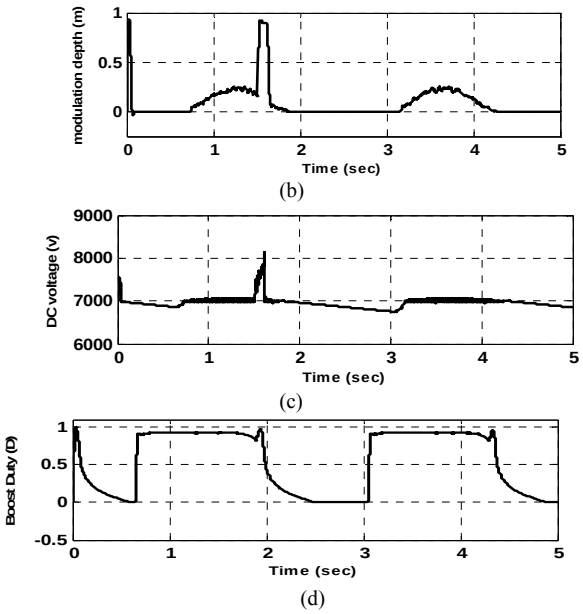

Fig.9: Dynamic response of power conditioning system variables for 3-phase fault 5 km from PV-PCC (a) instantaneous inverter voltage (b) modulation index (c) Dc-link voltage (d) duty cycle of boost converter.

6. CONCLUSIONS

The paper presents an integration of wind energy conversion system and PV arrayto micro-grid for efficient renewable energy utilization as clean source of electricity. The micro-grid integrated scheme consists also of boost converter, three phase voltage source inverter as two stage power conditioning system for PV array to enhance the system interface under different operation conditions. A simple MPPT constant voltage control is proposed using PI controller for directly forwarding the duty cycle to the boost converter. The inverter PI controller is suggested to control the dc link voltage faster and to have the output voltage equal to the grid voltage. The integrated system is digitally simulated and validated using the Matlab/Simulink. A detailed mathematical model of a three-phase grid-connected PV array and wind energy conversion system for MG applications has been proposed. The proposed model of the PV array and wind turbine uses theoretical and empirical equations together with data provided by the manufacturers. Dynamic system simulation studies demonstrate the effectiveness of the proposed control approaches and the detailed models presented under short circuit fault condition and solar radiation as well as wind speed variations. The PI controllers were tuned to improve the dynamic behavior of the system, fast recover of reactive power and increase the ability to withstand severe disturbances. The obtained results indicated that the proposed control scheme maintains voltage and PV power close to their nominal values for varying loads and climate conditions.

References:

[1] W. Shouxiang, W. Hui, C. Shengxia. “A Review of Optimization Allocation of Distributed Generations Embedded in Power Grid” Automation of Electric Power Systems. 2009(18), pp 110-115.

[2] F. D. Kanellos, N. D. Hatziargyriou, "The Effect Of Variable Speed Wind Turbines On The Operation Of Weak Distribution Networks," IEEE Trans. Energy Conversion, vol. 17, pp.543-548, Dec. 2002

[3] W. Chengshan, W. Shouxiang. “Study on Some Key Problems Related to Distributed Generation Systems”. Automation of Electric Power Systems. 2008(20), pp.1-4.

[4] J. A. P. Lopes, C. L. Moreira and A. G. Madureira, “De-fining Control Strategies for Micro Grids Islanded Operation,” IEEE Transactions on Power System, Vol. 21, No. 2, 2006, pp. 916-924.

[5] S. Barsali, et al., “Control Techniques of Dispersed Generators to Improve the Continuity of Electricity Supply,” IEEE Power Engineering Society Winter Meeting, New York, Vol. 2, 2002, pp. 789-794.

[6] E. Muljadim, C.P. Butterfield, "Pitch-Controlled Variable-Speed Wind Turbine Generation", IEEE Industry Applications Society Annual Meeting ,Phoenix, Arizona, October 3-7, 1999.

[7] A.D. Hansen, P. Sørensen, L. H. Hansen and H. Bindner, "Models for a Stand-Alone PV System, "Risø National Laboratory, Roskidle, Tech. Rep. Risø-R-1219 (EN)/SEC-R-12, Dec. 2000.

[8] K. H. Hussein, I. Muta, T. Hoshino, M. Osakada, "Maximum Photovoltaic Power Tracking: An Algorithm For Rapidly Changing Atmospheric Conditions", IEE Proc. Gener. Transm. And Distrib, Vol. 142, pp.59-64, Jan. 1995.

[9] C. Prapanavarat, M. Barnes and N. Jenkins, "Investigation Of The Performance of a Photovoltaic Ac Module," IEE Proc.-Gener. Transm. And Distrib, vol. 149, pp. 472-478, July 2002.

[10] H. Ibrahim, A. Ilinca and J. Perron, “Energy Storage Systems–Characteristics and Comparisons”, *Elsevier Renewable &Sustainable Energy Reviews*, Vol. 12, pp. 1221-1250, 2008.

[11] Ahmed S. Khalifa, Ihab F. El-Saadany,“Control of three phase grid connected Photovoltaic array with open loop maximum power point tracking”, IEEE PES General Meeting, July 26-29, 2011 Detroit, MI, USA.

[12] D. P.Hohmand , M. E. Ropp, “Comparative Study of Maximum Power Point Tracking Algorithms,” Progress in Photovoltaic Research and Applications, vol. 11, no. 1, pp. 47–62, 2003.

[13] W. Libo, Z. Zhengming, and L. Jianzheng, “A Single-Stage Three-Phase Grid-Connected Photovoltaic System With Modified MPPT Method and Reactive Power Compensation,” IEEE Transactions on Energy Conversion, vol. 22, no. 4, pp. 881–886,2007.

[14] LI Wei, Luc-Andre Gregoire, J. Bélanger,” Control and Performance of a Modular Multilevel Converter System”, CIGRÉ Canada Conference on Power Systems Halifax, September 6- 8, 2011.